

COMMUNICATION

A soft-templated method to synthesize sintering-resistant Au–mesoporous-silica core–shell nanocatalysts with sub-5 nm single-cores†

Cite this: *Chem. Commun.*, 2013, **49**, 3215

Received 25th December 2012,
Accepted 26th February 2013

DOI: 10.1039/c3cc39202c

www.rsc.org/chemcomm

Chunzheng Wu,^{ab} Zi-Yian Lim,^a Chen Zhou,^a Wei Guo Wang,^a Shenghu Zhou,^a Hongfeng Yin^{*a} and Yuejin Zhu^b

Nano-gold (sub-5 nm)@mesoporous-silica (m-SiO₂) core–shell nanospheres with controlled size and core number were prepared via a soft-templated method. The single-core Au@m-SiO₂ particles showed great sintering-resistance at 750 °C and kept high catalytic activity for CO oxidation after the treatment.

Oxide-supported gold nanocatalysts have become a hot research topic in recent years, and their preparation, properties and modification have been intensively investigated.¹ Due to their high activity in CO oxidation² and oxygen reduction,³ gold catalysts have been proposed to be promising candidates in pollution treatment and organic synthesis. However, gold catalysts tend to sinter at moderate-to-high temperatures during pretreatment and the catalytic process, which is an unsolved primary drawback for their applications in industry.

Synthesizing core–shell structures has been extensively considered as an efficient and promising strategy to prevent agglomeration of metal nanoparticles.⁴ The composite particles are designed to encapsulate active cores with various highly porous shells to acquire convenient substrate transpass as well as satisfactory isolation of nanoparticles. Typically, SiO₂,⁵ ZrO₂,⁶ Al₂O₃,⁷ Fe₂O₃⁸ and TiO₂⁹ have been reported as the shell materials. Among them, amorphous SiO₂ was the most widely adopted due to its high thermal stability, controllable morphology and desirable surface area. Most of the metal-cluster@SiO₂ spheres were prepared by water-in-oil microemulsion methods,^{5a,b,10} which were inconvenient and the particles always had limited porosities (with BET surface areas no more than 250 m² g⁻¹). The encapsulations of metal clusters by mesoporous SiO₂ shells with high surface areas were still less highlighted, and the cores were generally larger than those prepared by water-in-oil methods. Au particles of more than 15 nm were embedded into mesoporous SiO₂ shells by Corma¹¹ and Ostafin,¹² respectively,

yet no catalytic data were reported. To obtain smaller Au cores for active CO oxidation catalysts, approaches, such as coating on smaller metal colloids or etching of large Au cores, have been proposed.^{6b,13} However, the exact control of the core size by etching methods was found to be difficult, especially in the sub-10 nm range.¹⁴ Recently, Pt@m-SiO₂ nanocatalysts were prepared using the as-synthesized Pt colloids by Yang's group^{5c} and the core size could be controlled to 8.5 nm. Smaller (sub-5 nm) metal colloids such as Ag¹⁵ and Pt¹⁶ have also been engaged in mesoporous SiO₂ nanospheres, but the metal clusters were not effectively isolated during the SiO₂-coating process, and agglomerated-core¹⁵ or multi-core¹⁶ nanoparticles were formed unavoidably. Inspired by these studies, we focused on the preparation of single-core Au@m-SiO₂ nanoparticles with sub-5 nm Au cores and controlled shell thickness. Compared with the agglomerated-core and multi-core particles, the single-core structure possesses adequate and controllable distance between Au particles.

In this communication, a soft-templated method was adopted to synthesize the Au@m-SiO₂ nanoparticles. Firstly, gold colloids were prepared by reducing HAuCl₄ in the presence of tetradecyltrimethylammonium bromide (TTAB) as a stabilizer; secondly, SiO₂ shells were coated on the surface of the Au nanoparticles by the hydrolysis and polymerization of TEOS with TTAB micelles as mesopore templates; finally, the TTAB surfactants were removed by calcining the as-synthesized Au@TTAB-SiO₂ nanoparticles to form mesoporous SiO₂ shells.

The single-core Au@TTAB-SiO₂ particles shown in Fig. 1a and Fig. S2 (ESI†) had uniform spherical morphology with an average diameter of 42 nm. Gold cores of 3.2 nm were slightly larger compared with the as-synthesized colloids (2.5 nm, Fig. S1, ESI†), possibly due to the statistical neglect of some unobservable small gold particles in the shells. After calcining at 550 °C for 3 hours, TTAB micelle templates were removed (Fig. S3, ESI†) and mesopores of 2.0–2.7 nm could be observed in SiO₂ shells (Fig. 1b, inset). The BET surface area and total pore volume, analyzed by the nitrogen physisorption (Fig. 1d), were 736 m² g⁻¹ and 0.92 cm³ g⁻¹, respectively (Table S4, ESI†). The wormhole-like mesopores had a size distribution of

^a Division of Fuel Cell & Energy Technology, Ningbo Institute of Material Technology and Engineering, Chinese Academy of Sciences, Ningbo 315201, China. E-mail: yinhf@nimte.ac.cn; Fax: +86 574 8668 5846; Tel: +86 574 8668 5139

^b Department of Physics, Ningbo University, Ningbo 315211, China

† Electronic supplementary information (ESI) available. See DOI: 10.1039/c3cc39202c

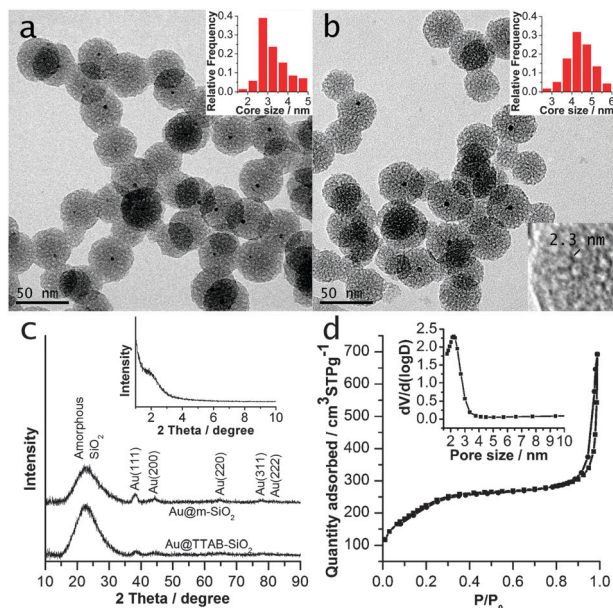


Fig. 1 TEM images of (a) Au@TTAB-SiO₂ nanoparticles and (b) Au@m-SiO₂ nanoparticles. (c) XRD patterns of Au@TTAB-SiO₂ and Au@m-SiO₂ nanoparticles, (d) N₂ sorption isotherms and pore size distribution of Au@m-SiO₂ nanoparticles obtained after the removal of TTAB.

approximately 2.2 nm calculated by the BJH method (Fig. 1d), and their structure lacked long-range order judging by the weak diffraction shoulder peak appearing at 2.0° in the low angle XRD patterns (Fig. 1c).¹⁶ Core-shell structure was widely retained after calcining, yet the average core size increased to 4.4 nm and the percentage of sub-3.5 nm Au particles dropped severely. It was proposed to be the result of Ostwald ripening.¹⁷ During the calcination, surface atoms of metal nanoparticles were able to diffuse even well below their melting point.¹⁸ Au atoms were emitted from the immobile Au cores as gas phase, transformed through the mesoporous shells and redeposited on nearby larger Au cores, which unavoidably resulted in the size change.

A novel synthesis strategy for single-core@mesoporous-shell structure was adopted in our work (Fig. 2). In the synthesis, SiO₂ nanospheres in the absence of gold cores could be formed by the hydrolysis and polymerization of TEOS with TTAB templates.

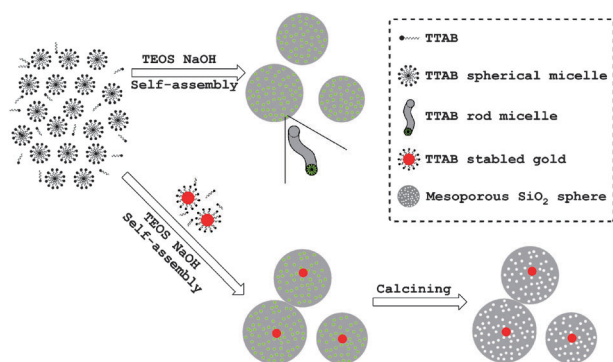


Fig. 2 The scheme of the formation procedures of mesoporous silica nanospheres when gold particles were absent or present.

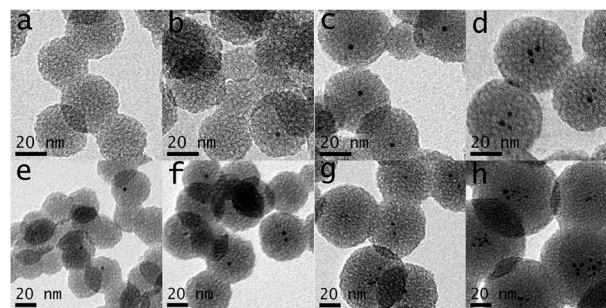


Fig. 3 TEM images of the Au@TTAB-SiO₂ nanoparticles obtained at a pH value of 11.4 with different gold concentrations: (a) 0 mM, (b) 0.067 mM, (c) 0.100 mM, (d) 0.167 mM. TEM images of the Au@TTAB-SiO₂ nanoparticles obtained at a gold concentration of 0.100 mM at different pH values: (e) 11.1, (f) 11.5, (g) 11.7, (h) 11.8.

The SiO₂ spheres had mesopore channels after calcining, which were templated by the self-assembled TTAB rod micelles as demonstrated in the synthesis of MCM-41.¹⁹ When TTAB-capped gold nanoparticles were present in the silica forming process, they were embedded inside the SiO₂ spheres instead of being supported on their surface. Upon increasing the gold particle concentration, the obtained SiO₂ spheres ranged from core-less to multi-core with a slight increase in sphere size for the occupancy of gold particles (Fig. 3a-d). According to the results, the formation of SiO₂ spheres was independent of the gold colloids, and the gold particles were “assigned” to the SiO₂ spheres equally. Thus, single-core particles were achieved when the gold particle concentration was close to that of the SiO₂ spheres. It is notable that despite the range of gold concentrations, an appropriate TTAB concentration (3.33–4.17 mM) was required to achieve the monodisperse spherical nanostructure (Fig. S5, ESI[†]).

The size and the number of SiO₂ spheres could be controlled by adjusting the pH values. Upon decreasing the pH value from 11.4 to 11.1, the SiO₂ sphere size dropped from 42 nm to 34 nm; meanwhile, core-less nanoparticles formed widely (Fig. 3e). In contrast, increasing the pH value resulted in larger spheres with multiple cores (Fig. 3f-h). It was suggested that a higher pH value leads to a lower number of SiO₂ spheres, with a higher number ratio of Au particles to SiO₂ spheres as well as larger SiO₂ sphere size. Accordingly, single-core particles of larger than 42 nm could be achieved by increasing the pH value and lowering the Au concentration (Fig. S8, ESI[†]).

Thinner SiO₂ shells were found to be available upon reducing TEOS concentration (Fig. S9a, ESI[†]), which would not lead to the appearance of core-less particles. Upon tuning the TEOS concentration, the SiO₂ sphere size changed while the core number was retained (Fig. S9, ESI[†]).

For the catalytic activity test towards CO oxidation, the Au@m-SiO₂ particles of ~30 nm and 2.9 wt% gold loading were used. As shown in Fig. 4a, a significant conversion of CO was detected at room temperature and the turnover frequency at 50 °C was 0.35 mol_{CO}g_{Au}⁻¹ h⁻¹, which was comparable with that of the highly active Au/SiO₂ particles prepared by CVD²⁰ and one order larger than those supported on mesoporous silica materials.²¹ Whereas, a decrease in the conversion was

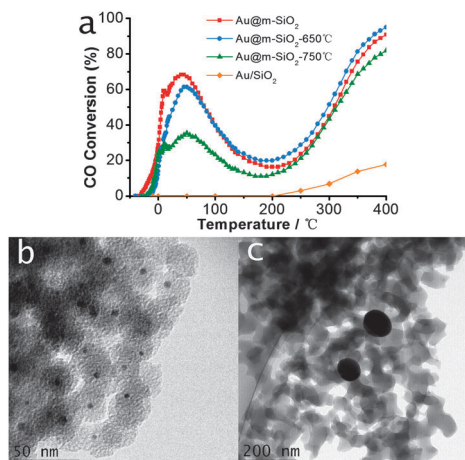


Fig. 4 (a) CO conversion of single-core Au@m-SiO₂ particles and supported Au/SiO₂ catalysts both with 2.9 wt% Au. TEM images of (b) Au@m-SiO₂ particles after the treatment at 750 °C and (c) supported Au/SiO₂ after calcining at 550 °C.

observed when the catalyst bed temperature was over 50 °C. Similar phenomena were also reported by Haruta²² and Zhu.²³ The activity drop was considered to be because of the loss of moisture (which could activate the inert SiO₂) with increasing temperature.²² The particles with larger size (42 nm) were surprisingly found to be more active than the smaller ones (30 nm, Fig. S10, ESI[†]). It was suggested that the mesoporous SiO₂ shell acted as more than a protector, it could influence the activity of gold possibly by enriching water vapor or reactants inside the shell. Further investigation into the catalytic mechanism is underway.

To investigate the thermal stability of catalysts, the Au@m-SiO₂ particles were further calcined at 650 °C and 750 °C, respectively. The CO conversion of the particles calcined at 750 °C showed an obvious decrease before 200 °C compared with the fresh and 650 °C calcined particles. However, the tendencies of light off curves after 200 °C were similar. Both the samples maintained the core-shell structure (Fig. S11d and e, ESI[†]) with no evident loss of BET surface areas (Fig. S12, ESI[†]), and the retained mesopores guaranteed the unimpeded mass transfer. The average core size of the 650 °C treated particles (4.7 nm) was close to the original (4.6 nm), while the cores of the 750 °C treated particles were slightly larger (5.1 nm), which may be responsible for the loss of the activity.

A supported catalyst was prepared by mixing amorphous SiO₂ with the as-synthesized Au colloids and evaporating the aqueous solvent at 50 °C. Without SiO₂ shells, the gold particles grew larger during the heating and concentrating process (~6.1 nm, Fig. S11f, ESI[†]) and sintered to several tens of nm after the calcination at 550 °C (Fig. 4c). As a result, no CO conversion was observed until 250 °C.

In summary, Au@m-SiO₂ core-shell nanoparticles with sub-5 nm cores were prepared *via* a TTAB-templated method. Single-core structure was obtained by tuning both the gold concentration and the pH value, and the shell thickness was controllable by TEOS concentration. The Au@m-SiO₂ showed high activity for CO oxidation at room temperature attributable to the small gold size and convenient mass pass. The SiO₂ shell

not only prevented the Au particles from migrating and coalescing but also limited their growth. After calcining at 750 °C, the Au@m-SiO₂ core-shell nanoparticles kept their structures and stayed active for CO oxidation at room temperature. It is of great meaning to develop such a sintering-resistant structure and preparation method, which is possible to be extended to other metals and high-temperature reactions.

This work is supported by the National Basic Research Program of China (2013CB934800), National Natural Science Foundation of China (Grant 21103212) and China Postdoctoral Science Foundation (2012M521208).

Notes and references

- (a) M. Haruta, *CATTECH*, 2002, **6**, 102–115; (b) G. J. Hutchings, *Catal. Today*, 2005, **100**, 55–61.
- M. Haruta, N. Yamada, T. Kobayashi and S. Iijima, *J. Catal.*, 1989, **115**, 301–309.
- (a) Y. Lee, A. Loew and S. Sun, *Chem. Mater.*, 2010, **22**, 755–761; (b) Q. Fu, A. Weber and M. Flytzani-Stephanopoulos, *Catal. Lett.*, 2001, **77**, 87–95.
- (a) Z. Ma and S. Dai, *ACS Catal.*, 2011, **1**, 805–818; (b) J. Liu, S. Z. Qiao, J. S. Chen, X. W. Lou, X. Xing and G. Q. Lu, *Chem. Commun.*, 2011, **47**, 12578–12591; (c) J. Liu, H. Q. Yang, F. Kleitz, Z. G. Chen, T. Yang, E. Strounina, G. Q. Lu and S. Z. Qiao, *Adv. Funct. Mater.*, 2012, **22**, 591–599.
- (a) J.-N. Park, A. J. Forman, W. Tang, J. Cheng, Y.-S. Hu, H. Lin and E. W. McFarland, *Small*, 2008, **4**, 1694–1697; (b) H.-L. Jiang, T. Umegaki, T. Akita, X.-B. Zhang, M. Haruta and Q. Xu, *Chem.-Eur. J.*, 2010, **16**, 3132–3137; (c) S. H. Joo, J. Y. Park, C.-K. Tsung, Y. Yamada, P. Yang and G. A. Somorjai, *Nat. Mater.*, 2009, **8**, 126–131.
- (a) P. M. Arnal, M. Comotti and F. Schüth, *Angew. Chemie., Int. Ed.*, 2006, **45**, 8224–8227; (b) X. Huang, C. Guo, L. Zuo, N. Zheng and G. D. Stucky, *Small*, 2009, **5**, 361–365.
- T. Montini, A. M. Condò, N. Hickey, F. C. Lovey, L. De Rogatis, P. Fornasiero and M. Graziani, *Appl. Catal., B*, 2007, **73**, 84–97.
- H. Yin, Z. Ma, M. Chi and S. Dai, *Catal. Today*, 2011, **160**, 87–95.
- I. Lee, J. B. Joo, Y. Yin and F. Zaera, *Angew. Chem., Int. Ed.*, 2011, **50**, 10208–10211.
- (a) D. S. Bae, K. S. Han and J. H. Adair, *J. Mater. Chem.*, 2002, **12**, 3117–3120; (b) M. Ikeda, T. Tago, M. Kishida and K. Wakabayashi, *Chem. Commun.*, 2001, 2512–2513.
- P. Botella, A. Corma and M. T. Navarro, *Chem. Mater.*, 2007, **19**, 1979–1983.
- R. I. Nooney, D. Thirunavukkarasu, Y. M. Chen, R. Josephs and A. E. Ostafin, *Langmuir*, 2003, **19**, 7628–7637.
- J. Lee, J. C. Park and H. Song, *Adv. Mater.*, 2008, **20**, 1523–1528.
- R. Güttel, M. Paul and F. Schüth, *Chem. Commun.*, 2010, **46**, 895–897.
- L. Han, H. Wei, B. Tu and D. Zhao, *Chem. Commun.*, 2011, **47**, 8536–8538.
- K. J. Lin, L. J. Chen, M. R. Prasad and C. Y. Cheng, *Adv. Mater.*, 2004, **16**, 1845–1849.
- S. B. Simonsen, I. Chorkendorff, S. Dahl, M. Skoglundh, J. Sehested and S. Helveg, *J. Catal.*, 2011, **281**, 147–155.
- X. H. Huang, Z. Y. Zhan, X. Wang, Z. Zhang, G. Z. Xing, D. L. Guo, D. P. Leusink, L. X. Zheng and T. Wu, *Appl. Phys. Lett.*, 2010, **97**, 203112.
- C. T. Kresge, M. E. Leonowicz, W. J. Roth, J. C. Vartuli and J. S. Beck, *Nature*, 1992, **359**, 710–712.
- M. Okumura, S. Nakamura, S. Tsubota, T. Nakamura, M. Azuma and M. Haruta, *Catal. Lett.*, 1998, **51**, 53–58.
- (a) C. M. Yang, M. Kalwei, F. Schüth and K. J. Chao, *Appl. Catal., A*, 2003, **254**, 289–296; (b) Y. S. Chi, H. P. Lin and C. Y. Mou, *Appl. Catal., A*, 2005, **284**, 199–206.
- M. Daté, M. Okumura, S. Tsubota and M. Haruta, *Angew. Chem., Int. Ed.*, 2004, **43**, 2129–2132.
- H. Zhu, Z. Ma, J. C. Clark, Z. Pan, S. H. Overbury and S. Dai, *Appl. Catal., A*, 2007, **326**, 89–99.